ELSEVIER

Journal of Alloys and Compounds 253–254 (1997) 642–647

Journal of ALLOYS AND COMPOUNDS

The influence of Co and various additives on the performance of $MmNi_{4.3-x}Mn_{0.33}Al_{0.4}Co_x$ hydrogen storage alloys and Ni/MH prismatic sealed cells

J.M. Cocciantelli[a,*], P. Bernard[b], S. Fernandez[a], J. Atkin[a]

[a]*SAFT, DTAI, 111 Bld A. Daney, 33074, Bordeaux, France*
[b]*SAFT Research, Route de Nozay, 91460, Marcoussis, France*

Abstract

$MmNi_5$ substituted alloys with Mn, Al and Co were studied as active materials for (−) electrodes in Ni/MH prismatic sealed cells for electric vehicles. In order to reduce the alloy cost, the influence of Co content was studied from 10–5% by weight in the AB_5 . As Co content is reduced, decrepitation and alloy corrosion are higher. Particularly, we showed how Al released by the corroded alloy polluted the (+) electrodes in the cell. Substitution of Co by Fe allows cost reduction without affecting Ni/MH cell performances and this behaviour is attributed to less decrepitation.

Keywords: Metal-hydride batteries; AB_5 alloy Co content; Cycle life; Al effect on the (+) electrode

1. Introduction

Ni/MH batteries are good candidates for E.V. batteries because of their high specific energy and energy density. They are also environmentally friendly and they meet the USABC mid-term performance criteria.

AB_5 alloys containing 10% in weight of expensive Co are now widely found in (−) MH electrodes of portable Ni/MH sealed cells because of their good electrochemical capacity and cycle life [1]. However alloy cost, and, particularly, alloy Co content, must be reduced.

This paper examines the influence of the Co content in $MmNi_{4.3-x}Mn_{0.33}Al_{0.4}Co_x$ (x=0.38, 0.51 and 0.72) on electrochemical characteristics and cycle life for Ni/MH 10 A h prismatic sealed cells. The effect of Cr and Fe addition was also studied.

2. Experimental

2.1. Preparation of alloys powder and evaluation

Alloy ingots were prepared by melting Mm, Ni, Co, Al and Mn in an induction-heating furnace, annealed in an argon atmosphere, then mechanically ground into a powder of 45 μm mean diameter. Pressure-composition isotherms were measured at 60 °C with a Sievert type apparatus. Incoming electrochemical inspection tests were performed for alloys in half cell with 8.7 N KOH electrolyte. To test the alloy, 1 g of powder was mixed with 0.3 g of Ni powder and compressed between two layers of Ni foam to obtain a pellet (−) electrode. 7 h 30 min C/5 charge and C/5 discharge to −750 mV with respect to the Hg/HgO (reference electrode) were performed for capacity evaluation followed by 40 °C C rate with 80% DoD and a 0.08 overcharge abusive cycling for accelerated alloy cycle life evaluation.

2.2. Evaluation of alloys in sealed cells

The alloy powder was mixed in a paste with cellulosic thickener, carbone and styrene butadiene binder then applied into a nickel foam substrate dried and compressed to obtain (−) MH electrodes. Six of these flat electrodes were combined with 5 foam (+) electrodes containing $Ni_{1-x-y}Co_xZn_y(OH)_2$, Co and $Co(OH)_2$, using an appropriate separator. 10 A h, (+) limited prismatic sealed cells, were made. These cells were evaluated using 7 h 30 min C/5 charge followed by C/3 or C rate discharge to 1 V. Cycling was performed at a C/3 rate charge with a 0.15 overcharge coefficient and a C rate 80% DoD discharge. Internal pressure, capacity and half-discharge voltage were measured during cycling. Failure analysis was performed by dismantling cells and measuring electrode capacities in

*Corresponding author.

0925-8388/97/$17.00
PII S0925-8388(96)02978-7

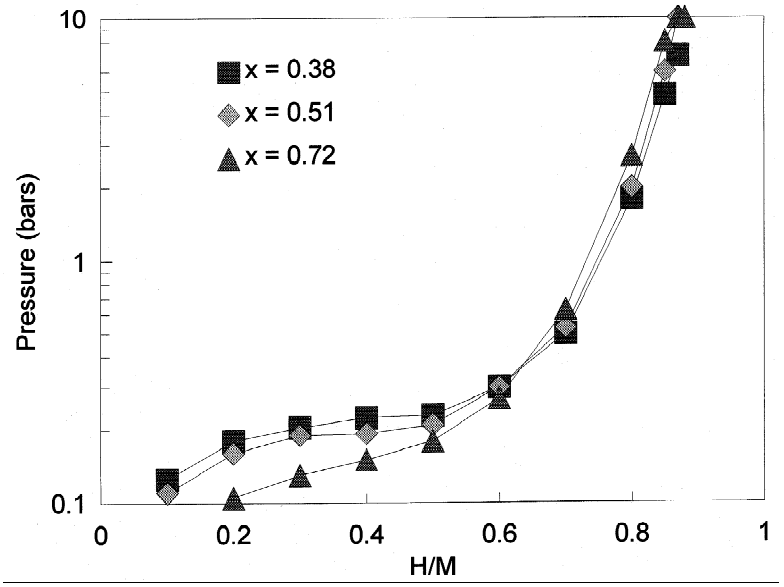

Fig. 1. PCI at 60 °C for $MmNi_{4.3-x}Mn_{0.33}Al_{0.4}Co_x$ alloys.

flooded cells at C/5 to −750 mV for (−) and 150 mV for (+) at 20 °C with respect to Hg/HgO.

3. Results and discussion

3.1. Incoming inspection tests for alloys

Fig. 1 shows PCI measurements for $MmNi_{4.3-x}Mn_{0.33}Al_{0.4}Co_x$ alloys with $x=0.72$, 0.51 and 0.38. Comparable solid–gas absorption capacities of 330 mA h g^{-1} are obtained at 10 bars. Pressure decreases with increasing Co content as already mentioned for $LaNi_{5-x}Co_x$ [2].

Incoming inspection tests and abusive cycling at 40 °C were carried out for various alloys. Fig. 2 shows alloy capacity and changes during cycling. Analysis revealed higher decrepitation for low Co content (20 μm, 15 μm and 5 μm mean grain size after 400 cycles, respectively, for $x=0.72$, 0.51 and 0.38) and X-ray diffractograms of alloys showed peaks characteristics for rare earth hydroxides, particularly for $x=0.38$.

The higher decrepitation for low Co content seems to be correlated with higher $\Delta V/V$ during α to β phase transformation [3]; in fact we measured, using X-ray diffraction after H_2 solid–gas absorption, $\Delta V/V=9.1\%$ and 12% at 2.4 H/M, respectively, for $x=0.72$ and $x=0.38$. Volume expansion induces internal stress which is released by pulverization [4].

In order to determine the role of Co on alloy surface

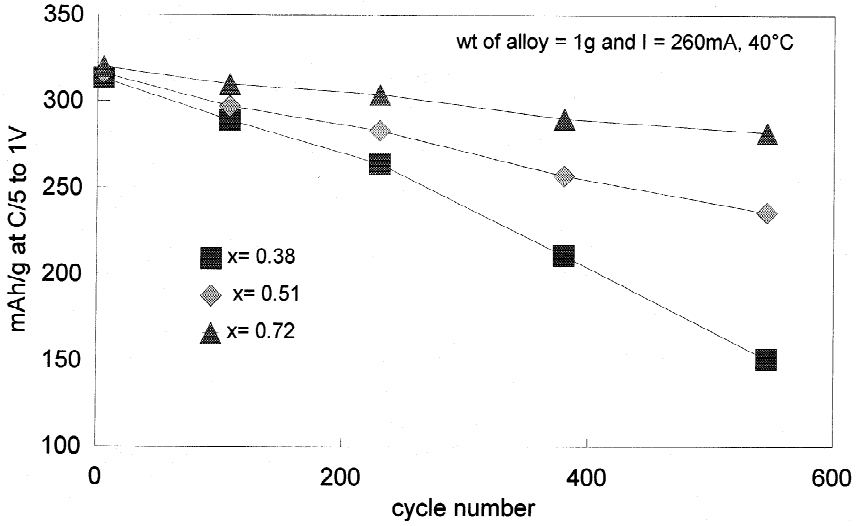

Fig. 2. C/5 capacity evolution with abusive cycling for $MmNi_{4.3-x}Mn_{0.33}Al_{0.4}Co_x$ alloys ($x=0.38$, 0.51 and 0.72).

corrosion, we soaked 10 g of each of these powders in 33 ml of stirred 8.5 N electrolyte for 24 h at 70 °C. We measured Al in the electrolyte as an indicator of alloy corrosion, indeed Mn and Co have low solubilities and rare earth hydroxides have very low solubilities and reprecipitate on the alloy surface [5].

For $x=0.72$ and $x=0.38$ we found, respectively, 60 and 100 mg of Al per l of electrolyte, showing that the Co content has an influence on the surface oxidation rate.

The reason why $\Delta V/V$ and corrosion changes with Co content is not clear. Particular attention must be focused on the relation between the alloy Co content and the length of its β solid solution domain [6].

In order to stabilize performances of low Co content AB_5 we decided to introduce transition-metal elements which seem beneficial for life: Cr in the case of $LaNi_{5-x}M_x$ alloys [4] and Fe in the case of $MmNi_{3.6}Fe_{0.7}Al_{0.3}Mn_{0.4}$ [7].

Fe substitution must be adjusted to avoid a too low initial capacity and voltage for electrode [8]; hence, we manufactured $MmNi_{3.93-x}Mn_{0.33}Al_{0.4}Co_{0.37}M_x$ with $x=0.15$ for Fe and Cr. Fig. 3 shows alloy capacity and its change with cycling. We noted the effect of Fe on capacity during cycling.

3.2. Evaluation of alloys in 10 A h Ni/MH sealed cells

In order to understand the influence of AB_5 alloy Co content in 10 A h Ni/MH prismatic sealed cells we decided to run a first experiment with $MmNi_{4.3-x}Mn_{0.33}Al_{0.4}Co_x$ alloys ($x=0.72$, 0.51 and 0.38).

As shown in Fig. 4, cell capacity decreased as the Co content decreased, while the internal pressure increased.

C rate half discharge voltage is affected after cycling when using low-Co AB_5. This phenomenon is corrected when adding 10% more electrolyte to the cycled cells.

These results were explained after discharging cells to 1 V, dismantling them and analysing the (−) and (+) electrodes, as shown in Table 1.

Pressure evolution with cycling is attributed to the lowering of (−) capacity and to the increase of the discharge reserve (initially equal to 0). This last phenomenon, already mentioned in the case of portable Ni/MH sealed cells [9], was partially attributed to the corrosion of alloy, the cathodic reaction being water and/or O_2 reduction. H_2 gas analyzed at the end of the charge confirms this hypothesis.

According to Table 1 cell capacity change is attributed to the (+) electrode and unexpectedly to the Co content in the alloy in the (−) electrode.

3.3. Effect of Al on the (+) electrode

X-ray fluorescence and PCI measurements were performed on the positive electrodes. Lanthanum and cerium, which are known poisons for the nickel electrode [10], were particularly followed. For all the electrodes, an average value of 1 ppm of La and 0.1 ppm of Ce was measured on the surface; however, none of these elements has been detected inside the electrodes. The absence of these elements is not surprising, due to the very low level of solubility of La (10^{-22} M) and Ce (10^{-23} M) in alkaline solution.

The PCI measurements on the positive electrode showed the presence of Mn and Al, whose amounts are correlated with the amount of Co in the AB_5 alloy, as shown in Table 1. The higher the amount of Co in the alloy, the lower the amount of Al and Mn in the positive electrode.

According to these results, specific electrochemical tests

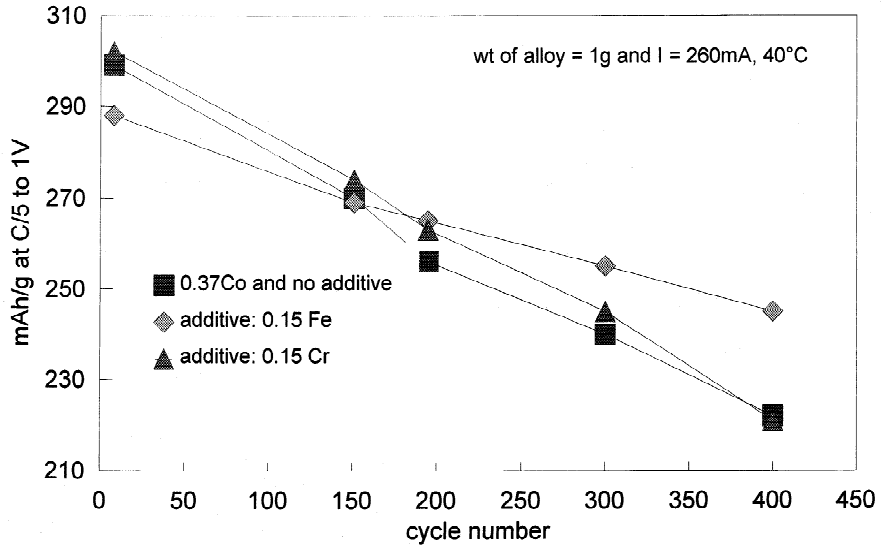

Fig. 3. C/5 capacity evolution with abusive cycling for $MmNi_{3.93-x}Mn_{0.33}Al_{0.4}Co_{0.37}M_x$ alloys (M=Cr and Fe).

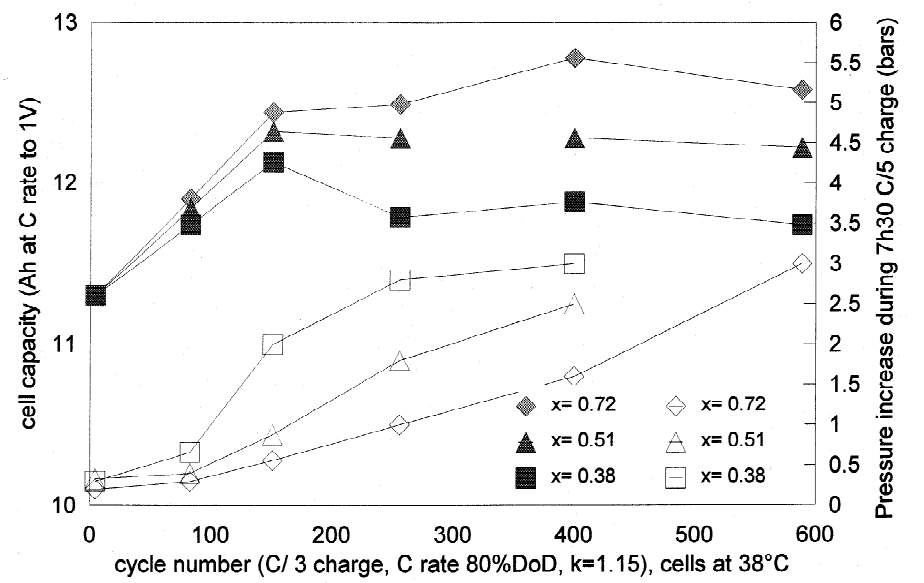

Fig. 4. 10 A h sealed cells capacity and cell inner pressure evolution with cycling for $MmNi_{4.3-x}Mn_{0.33}Al_{0.4}Co_x$ (x=0.38, 0.51 and 0.72).

Table 1
Characteristics of (+) and (−) electrodes after 400 cycles in 10 A h Ni/MH sealed cells

Nature of AB_5 in the Ni/MH cell	(−) reserve at 400 cycles (mA h g^{-1} of alloy)	(+) capacity (mA h g^{-1} of positive active material)	(−) capacity (mA h g^{-1} of alloy)	Al in (+) electrode (mg dm^{-2})	Mn in (+) electrode (mg dm^{-2})
Alloy with xCo=0.72	68	268	313	57	5
Alloy with xCo=0.51	99	260	299	75	7
Alloy with xCo=0.38	82	248	263	172	14

were performed by adding increasing amounts of MnO and $Al(OH)_3$ powders in positive foam electrodes, and testing them in NiCd flooded cells. The results are summarised in Table 2.

For the studied amount of MnO, it appears that the Mn does not influence the electrochemical yield of $Ni(OH)_2$. On the contrary, the addition of Al reduces dramatically the gravimetric efficiency of the (+) electrode. As shown in Fig. 5, the addition of Al induces the formation of a second discharge plateau at a higher voltage, the higher amount of Al, the longer the plateau. The length of this plateau increased during cycling.

X-ray analysis of the (+) electrode in the discharged state (Fig. 6) allowed us to understand better these phenomena.

Besides the peaks of the well known β_{II} $Ni(OH)_2$ structure, the characteristic peaks of an hydrotalcite-like α phase which can be indexed on a hexagonal cell (a=3.08 Å, c=22.8 Å) are observed [11].

The presence of this phase can be understood by the insertion of Al into the lattice of $Ni(OH)_2$ via a mechanism of dissolution–precipitation of the active material. Indeed, in the presence of Ni, Al and carbonate in alkaline solution, the precipitated phase becomes the hydrotalcite-like α phase stabilized by the aluminium. Furthermore, this compound is known to shift the peak potentials by about 50 to 70 mV to more anodic potentials compared with pure $Ni(OH)_2$ [12].

In brief, the loss of capacity of the positive electrode comes from the degradation of the chargeability due to the formation of hydrotalcite-like phase stabilized by the Al coming from the corrosion of the AB_5 alloys. This

Table 2
Efficiency of positive electrode containing MnO and $Al(OH)_3$

Additives incorporated in the (+) electrode	(no addition)	Al 85 mg dm^{-2}	Al 170 mg dm^{-2}	Al 450 mg dm^{-2}	Mn 4 mg dm^{-2}	Mn 17 mg dm^{-2}
Capacity of the (+) active material (mA h g^{-1})	281	237	228	220	282	280

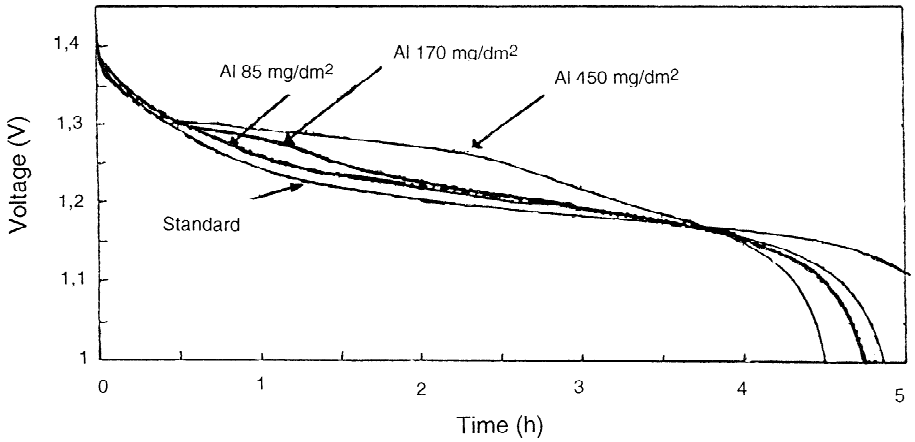

Fig. 5. Discharge curves of positive foam electrodes containing increasing amounts of $Al(OH)_3$, after 35 cycles.

hypothesis is confirmed by the X-ray diffraction diagrams of the positive electrode, where the characteristic peaks of the new phase are observable for the positive electrode with $x(Co)=0.38$ in the MH electrode.

3.4. Evaluation of 10 A h Ni/MH sealed cells, influence of Fe addition to 7% Co AB_5

In the last experiment we tried to confirm the relevance of Fe substitution for $MmNi_{3.8-x}Mn_{0.33}Al_{0.4}Co_{0.51}Fe_x$ ($x=$ 0 and 0.16) alloys. Fig. 7 shows the encouraging effect of Fe when looking at capacity and pressure evolution with cycling for 10 A h cells. The analyzed electrodes after 330 cycles revealed much more stable capacity for Fe-containing alloys, less discharge reserve capacity and less Al in the (+) electrodes, which explained their stable capacity.

The Al content is correlated with corrosion of the alloy; this was proved by oxygen LECO analysis, and, in fact, 3.2% of oxygen is contained in the Fe-substituted alloy compared to 5% without Fe. This first value is comparable with that obtained for the 10% Co AB_5. In these cases 80, 135 and 110 mg of Al per dm^2 of (+) electrode were found, respectively, for 7% Co+Fe, 7% Co and 10% Co content AB_5.

The SEM pictures revealed that, in a way similar to Co, Fe reduces the alloy decrepitation and results in two effects:

1. There is less surface area in contact with the electrolyte, and, therefore, less corrosion.
2. There is less reduction in particle size, and, therefore, better electrical conductivity, resulting in better performance during cycling.

As Fe is a poison for the (+) electrode, by affecting its

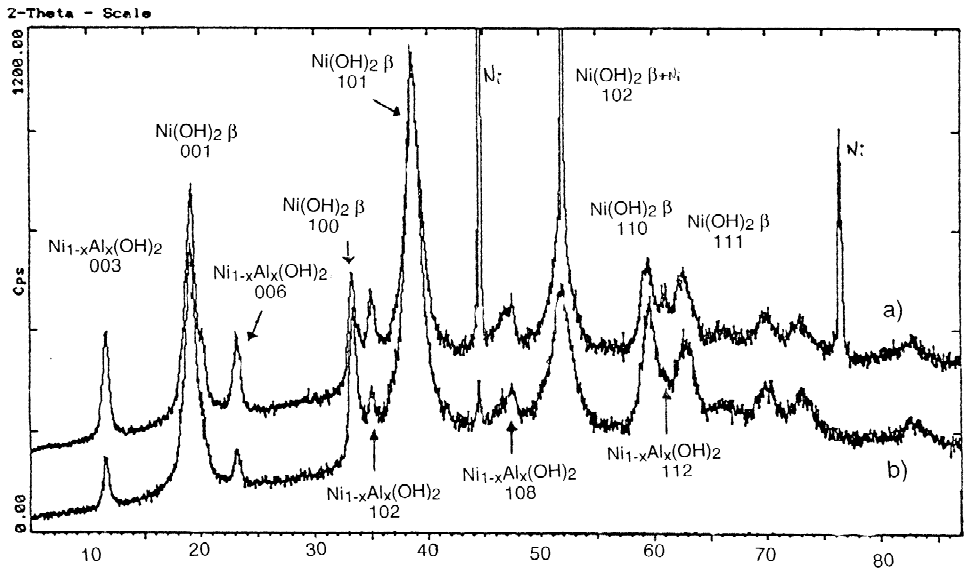

Fig. 6. XRD patterns of the positive electrode containing 170 mg dm^{-2} of Al, after 35 cycles. Discharged state: (a) surface, and (b) powder.

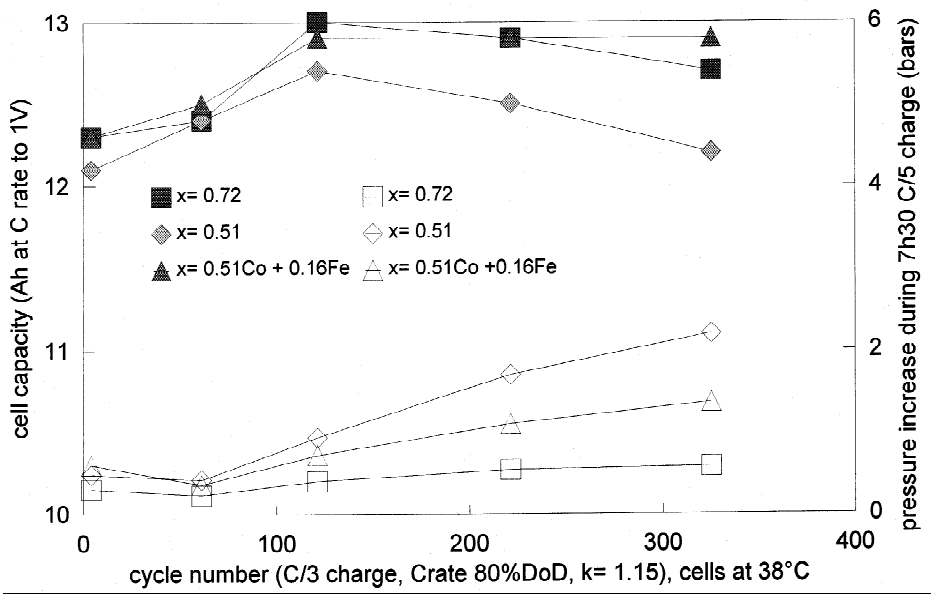

Fig. 7. 10 A h sealed cells capacity and cell inner pressure evolution with cycling for $MmNi_{4.3-x}Mn_{0.33}Al_{0.4}Co_x$ (x=0.51, 0.72 and 0.51Co+0.16Fe).

chargeability, we measured after 330 cycles 200 ppm of Fe, but no influence on the (+) electrode capacity was found when charging 10 A h cells at C/10 and 40 °C. In fact, this result must be compared with a standard cell (containing 10% Co AB_5 alloy) for which we found 150 ppm of Fe in the positive electrode.

4. Conclusions

Beyond the known effects of Co on the alloy performances, we demonstrated that reducing Co on the AB_5 from x=0.75 to x=0.38 decreased Ni/MH 10 A h cell cycle life. This is attributed to poisoning of the (+) electrode by Al, increased cell inner pressure and electrolyte consumption. Decrepitation of low Co content AB_5 seemed to be the main reason for these phenomena as it increased surface area and corrosion.

At the moment Fe seems to be a good candidate to reduce Co content in the alloy while avoiding decrepitation with cycling; cycle life and storage must now be carried out.

Other routes for Co content reduction must be explored such as stoichiometry increase (x>5), but also use of predecrepitated surface-treated powder in order to avoid corrosion and the release of poisoning elements into the sealed cells.

Acknowledgments

The authors would like to thank Dr. B. Knosp and Dr. P. Leblanc from Alcatel-Alsthom Research and SAFT Research Laboratories for $\Delta V/V$ measurements, Al analysis and SEM pictures for alloy powders after cycling. The authors would like also to thank Treibacher Auermet and Santoku Metal Industry Co. who graciously supplied various alloy samples tested in this paper.

References

[1] H. Ogawa, M. Ikoma, H. Kawano and I. Matsumoto, *J. Power Sources, 12* (1988) 393.
[2] H.H. Van Mal, K.H.J. Buschow and F.A. Kuijpers, *J. Less-Common Met., 32* (1973) 289.
[3] P.H.L. Notten, *NATO ASI Series E, 281* (1995) 151.
[4] T. Sakai, K. Oguro, H. Miyamura, N. Kuriyama, A. Kato, H. Ishikawa and T. Iwakura, *J. Less-Common Met., 161* (1990) 193.
[5] F. Meli, A. Zuettel and L. Schlapbach, *J. Less-Common Metals, 190* (1992) 17.
[6] M. Latroche, A. Percheron-Guegan, Y. Chabre, J. Bouet, J. Pannetier and E. Ressouche, *J. Alloys and Compounds, 231* (1995) 537.
[7] F. Meli, A. Zuettel and L. Schlapbach, *J. Alloys and Compounds, 231* (1995) 639.
[8] J. Lamloumi, C. Lartigue, A. Percheron-Guegan and J.C. Achard, *Rare Earths in Mod. Sc. and Tech.,* (1980) 563.
[9] H. Kaiya and T. Ookawa, *J. Alloys and Compounds, 231* (1995) 598.
[10] D.A. Corrigan and R.M. Bendert, *J. Electrochem. Soc., 136(3)* (1989) 723.
[11] P. Vishnu Kamath, M. Dixit, L. Indira, A.K. Shukla, V. Ganesh Kumar and N. Munichandraiah, *J. Electrochem. Soc., 141* (1994) 2956.
[12] L. Indira, M. Dixit and P. Kamath, *J. Power Sources, 52* (1994) 93.